WAVE PROPAGATION ANALYSIS IN SEMI-INFINITE DOMAIN USING AN INDIRECT BOUNDARY ELEMENT METHOD

Siamak H. KHOSHDEL[1], K. BARGI[2] and A. NOORZAD[3]

ABSTRACT: The scattering and diffraction of plane elastic waves (P-and SV-waves) by a canyon of arbitrary shape has been studied in this paper. Semi-infinite domain analysis under seismic waves is studied using an indirect boundary element method. According to advantages of BEM, the applied method can treat semi-infinity and arbitrary shape properties of the canyons. Then canyons with different shapes are analyzed under seismic P- and SV-waves with arbitrary frequencies and angle of incidences, and most important parameters are investigated. This approach applied in both frequency and time domain analyses. On the other hand, according to the concept of double layer potentials in mathematics, an indirect BEM with a fictitious boundary is applied and the singularity problem in direct BEM is diminished. In this proposed method, the placement of source and receiver points are separated. Case studies in time and frequency domains are derived and proper position for placing of the fictitious boundary is determined.

Key Words: Wave propagation, semi-infinite domain, fictions boundary

INTRODUCTION

The research on the two-dimensional elastic wave scattering by surface irregularity in an elastic and homogeneous medium is one of the most important parameters in design of some specific structures and has been interested for many years. According to importance of some huge structures like dams and bridges, it seems be necessary to evaluate the effects of surface irregularities on the free field ground motion during earthquake. The simplest problems are associated with incidence of plane SH waves. This case has been analyzed for different canyon shapes with closed form or numerical methods (Trifunac 1993 , Shah and Wong 1982 , Sanchez-Sesma and Rosenblueth 1974, and Lee 1978). Of course closed form methods could be applied just for regular and simple geometry of the topography, like semi-cylindrical and semi-elliptical shapes. The problems involving in-plane motion (P- and SV-waves) are more complicated because of the mode conversion during reflection from free ground surface. Some numerical solutions in the field of elastic wave propagation employing discrete analysis such as the finite difference method Boore 1972b and the finite element method Smith 1978, have been developed. These methods are domain methods, and even modelling a large body around the surface irregularity (according to available computer memory), radiation condition will not be obeyed simply and exactly.

In this paper, the boundary element method (BEM) is used for solving elastic wave propagation. Using this method, only the boundary surface of the semi-infinite domain needs to be modeled, and on

[1] Visiting Researcher, From Tehran University
[2] Professor., Tehran University
[3] Associate Prof., Tehran University

the other hand radiation condition will be obeyed automatically. Meanwhile, using a fictitious boundary, an indirect BEM is proposed for avoiding the singularity in the equations of ordinary BEM.

PROBLEM FORMULATION

The governing equation for an elastic, isotropic and homogeneous solid of volume V and surface $S=S_1+S_2$, is the Navier-Caushy equation as follows:

$$(\lambda+\mu)u_{i,ij}+\mu u_{j,ii}+\rho b_j=\rho\ddot{u}_j \tag{1}$$

where $u_i(x, t)$ is the displacement vector at point x and time t, b_j is the body force per unit mass, λ and μ are the Lame constants and ρ is the mass density. The Cartesian coordinate system $(i,j=1,2,3)$ is used here and the summation convention is implied for repeated indices. By defining the propagation velocities of the pressure and shear waves in the solid as follows:

$$C_1^2=(\lambda+2\mu)/\rho, and, C_2^2=\mu/\rho \tag{2}$$

Equation (1) can be written as:

$$(C_1^2-C_2^2)u_{i,ij}+C_2^2u_{j,ii}+b_j=\ddot{u}_j \tag{3}$$

Equations (1) and (3) must be accomplished by initial conditions:

$$u_i(x,0)=\overset{0}{u}_i,\dot{u}_i(x,0)=\overset{0}{v}_i \tag{4}$$

in V and boundary conditions

$$\begin{aligned} u_i(x,t)&=U_i, x\in S_1\\ t_i(x,t)&=\sigma_{ij}n_j=T_i, x\in S_2 \end{aligned} \tag{5}$$

on S, where t_i are the tractions, $n_j(x)$ is the outward normal vector and U_i and T_i are prescribed values for displacements and tractions, respectively. For a bulky solid whose cross-sectional area and loading remain constant along the x_3-direction (plane strain case), the following assumption is made:

$$\begin{aligned} u_1&=u_1(x_1, x_2, t)\\ u_2&=u_2(x_1, x_2, t)\\ u_3&=0 \end{aligned} \tag{6}$$

The governing equation of motion for this case will be as follows:

$$(\lambda+\mu)u_{\beta,\beta\alpha}+\mu u_{\alpha,\beta\beta}+\rho b_\alpha=\rho\ddot{u}_\alpha \tag{7}$$

where α, β, range from 1 to 2. It's the same as (1) except for the restricted range of the indices. On the other hand, for simplicity one can convert above equations from time to frequency domain. Application of the Laplace transform to the equations of motion (3) gives:

$$(C_1^2-C_2^2)\bar{u}_{i,ij}+C_2^2\bar{u}_{j,ii}+\bar{b}_j=s^2\bar{u}_j-s\overset{o}{u}_j-\overset{o}{v}_j \tag{8}$$

The above equation is an elliptic partial differential equation and more amenable to numerical treatment than the original one, which is of hyperbolic type. The solution of (8) is a function of the transform parameter s and must satisfy the transformed boundary conditions:

$$\begin{aligned} \bar{u}_i(x,s) &= \overline{U}_i \quad ,x \in S_1 \\ \bar{t}_i(x,s) &= \overline{\sigma}_{ij} n_j = \overline{T}_i \quad ,x \in S_2 \end{aligned} \tag{9}$$

Boundary Integral Equation

The mathematical basis for direct integral equation formulation in elastodynamic is the dynamic reciprocal theorem. It specifies a relationship between a pair of elastodynamic states. In fact, it is the dynamic extension of the classical reciprocal theorem of Betti-Rayleigh in elastostatics augmented by the inertia forces.

Consider two distinct elastodynamic states:

$$\begin{aligned} Condition - A &= [u_i, t_i, b_i] \\ Condition - B &= [u'_i, t'_i, b'_i] \end{aligned} \tag{10}$$

defined in that region and with initial conditions:

$$\begin{aligned} u_i(x,o) &= \overset{o}{u}_i(x) \quad ,u'_i(x,o) = \overset{o}{u'}_i(x) \\ \overset{o}{u}_i(x,o) &= \overset{o}{v}_i(x) \quad ,\overset{o}{u'}_i(x,o) = \overset{o}{v'}_i(x) \end{aligned} \tag{11}$$

Then, for t > 0 :

$$\begin{aligned} \therefore \int_S t_i * u'_i ds + \int_V \rho \left\{ b_i * u'_i + \overset{o}{v}_i u'_i + \overset{o}{u}_i \overset{o}{u'}_i \right\} dV = \\ \int_S t'_i * u_i ds + \int_V \rho \left\{ b'_i * u_i + \overset{o}{v'}_i u_i + \overset{o}{u'}_i \overset{o}{u}_i \right\} dV \end{aligned} \tag{12}$$

The operation * above denotes time convolution [7].

Fundamental Solutions

The fundamental singular solution at point x (receiver) for displacement component i due to a concentrated pulse at point ξ source) in direction j and in a three-dimensional elastic solid of infinite extent is the solution of Equation (3) with a body force:

$$b_j = \delta(x - \xi)\delta(t - \tau)e_j \tag{13}$$

Where δ denotes the Dirac delta function and e is a constant unit vector. The fundamental displacement singular solution in two dimensions for a unit impulse uniform distributed along the x_3 –axis is:

$$G_{ij}(x,t,\xi,\tau = 0) = (2\pi\rho)^{-1} \left\{ \left(\frac{\left[2t^2 - \frac{r^2}{c_1^2} \right]}{\left[t^2 - \frac{r^2}{c_1^2} \right]^{1/2}} H(t - \frac{r}{c_1}) - \frac{\left[2t^2 - \frac{r^2}{c_2^2} \right]}{\left[t^2 - \frac{r^2}{c_2^2} \right]^{1/2}} H(t - \frac{r}{c_2}) \right) \frac{r_\alpha r_\beta}{r^4} \right.$$

$$-\left[\left(t^2-\frac{r^2}{c^2_1}\right)^{1/2}H(t-\frac{r}{c_1})-(t^2-\frac{r^2}{c^2_2})^{1/2}H(t-\frac{r}{c_2})\right]\frac{\delta_{\alpha\beta}}{r^2}+\frac{1}{c^2_2\left[t^2-\frac{r^2}{c^2_2}\right]^{1/2}}H(t-\frac{r}{c_2})\delta_{\alpha\beta}\ \}$$

(14)

where, subscripts α, β ranges from 1 to 2 and H is the Heaviside function. The square brackets in (14) denote retarded time values. An expression for fundamental traction singular solution can be found using the relationship between traction and displacement solutions. It is preferable, however, to derive the two-dimensional fundamental solutions from their three-dimensional counterparts by numerically integrating the later in the x_3-direction as described in Manolis (1988) [7].

The fundamental singular solutions in the Laplace transformed domain for a point in a two-dimensional solid of infinite extent are [7,1]:

$$\overline{G}_{ij}(x,\xi,s)=(\xi\pi\rho C_2^2)^{-1}\left[\bar{a}\delta_{ij}-\bar{b}r_{,i}r_{,j}\right] \tag{15}$$

$$\begin{aligned}\overline{F}_{ij}(x,\xi,s)=(\xi\pi)^{-1}\{&(\bar{a}_{,r}-\bar{b}\,r^{-1})\left(\delta_{ij}\frac{\partial r}{\partial n}+r_{,j}n_i\right)-(2\bar{b}\,r^{-1})\left(n_jr_{,i}-2r_{,i}r_{,j}\frac{\partial r}{\partial n}\right)\\&-(2\bar{b}_{,r})\left(r_{,j}r_{,j}\frac{\partial r}{\partial n}\right)+(\bar{a}_{,r}-\bar{b}_{,r}-0.5\xi\bar{b}\,r^{-1})\left(\frac{C^2_1}{C^2_2}-2\right)(r_{,i}n_j)\}\end{aligned} \tag{16}$$

where:

$$\begin{cases}\bar{a}=K_0\left(\dfrac{sr}{C_2}\right)+\left(\dfrac{C_2}{sr}\right)\left\{K_1\left(\dfrac{sr}{C_2}\right)-\left(\dfrac{C_2}{C_1}\right)K_1\left(\dfrac{sr}{C_1}\right)\right\}\\ \bar{b}=K_2\left(\dfrac{sr}{C_2}\right)-\left(\dfrac{C_2^2}{C_1^2}\right)K_2\left(\dfrac{sr}{C_1}\right),\xi=2\end{cases} \tag{17}$$

$$with:\frac{\partial r}{\partial n}=\frac{\partial r}{\partial x_i}.\frac{\partial x_i}{\partial n}=r_{,i}n_i$$

where K_0, K_1 and K_2 are the modified Bessel functions of the second kind and of zero, first and second orders, respectively.

Integral Representation

Using the dynamic reciprocal theorem (12) with the unprimed state being the real one and the primed state being the fundamental singular solutions, Love's integral identity may be derived in the form [7,1]:

$$C_{ij}(\xi)u_j(\xi,t)=\int_S\left[G_{ij}*t_i(x,t)-F_{ij}*u_i(x,t)\right]dS(x)+\rho\int_V G_{ij}*b_i(x,t)dV(x)+\rho\int_V\left[G_{ij}\overset{0}{v}_i(x)+\dot{G}_{ij}\overset{0}{u}_i(x)\right]dV(x) \tag{18}$$

where, ξ and x are receiver and source points, respectively, and tensor C_{ij} can be expressed as:

$$C_{ij}=\delta_{ij}-\gamma_{ij} \tag{19}$$

where δ_{ij} is the Kronecker's delta and γ_{ij} is a discontinuity or jump term such that for ξ inside the region is equal to zero; for ξ exterior to the region is equal to δ_{ij} and for ξ on the boundary

is defined by the local tangent plane. For a smooth surface, that value is equal to $0.5\,\delta_{ij}$.

In transformed domains one can again has the appropriate extension of Betti's theorem for two transformed dynamic states. The integral representation in Laplace-transformed domain will be as follows:

$$C_{ij}(\xi)\bar{u}_i(\xi,s)=\int_S\{\bar{G}_{ij}\bar{t}_i(x,s)-\bar{F}_{ij}\bar{u}_i(x,s)\}dS(x)+\int_V\bar{G}_{ij}\bar{b}_i(x,s)dV(x) \qquad (20)$$

Fourier transformed domain representation can be derived from (20) by simply replacing s by $-i\omega$ if the initial conditions are zeros. Neglecting body forces and initial conditions for earthquake engineering problems, Equations (18) and (20) will convert to boundary integral equations; the integration will be done only on the surface of the domain.

For the purpose of integrating of Equations (18) and (20) one has to descritize the geometry (boundary surface) of the problem and the field variables (displacements and tractions). In this study, in order to develop accurate BEM algorithms, isoparametric representations of the geometry and problem parameters based on polynomial shape functions, quadratic elements with 3 nodes per element are used.

Then, the boundary integral equation (18) changes to:

$$C_{ij}u_i(\xi)=\sum_{q=1}^{Q}\int_{S_q}G_{ij}(x(\eta),\xi)M_\alpha(\eta)dS(x(\eta))T_{i\alpha}^n-\int_{S_q}F_{ij}(x(\eta),\xi)M_\alpha(\eta)dS(x(\eta))U_{i\alpha}^n \qquad (21)$$

where S_q is the surface of the qth element and Q is the total number of boundary elements needed to model the surfaces of the problem, η. is the intrinsic coordinate system, and T and U are nodal values of tractions and displacements, respectively.

A system of algebraic equations can be obtained at time step n (or frequency number n in frequency domain- Equation (20)), by allowing point ξ. to coincide sequentially with all the nodal points of the boundary. These linear equations in matrix form read:

$$[G]\{t\}^n=[F]\{u\}^n \qquad (22)$$

where $\{t\}^n$ and $\{u\}^n$ are nodal tractions and displacements, respectively. Also, [G] and [F] are coefficient matrices containing the contributions of surface integrals of the kernel-shape function products $G_{ij}M_\alpha$ and $F_{ij}M_\alpha$, respectively, and the free term C_{ij} contribution has been absorbed in [F]. In time domain analysis, calculating of [G] and [F] need deriving time-convolution integrals, while in transformed domain there are no convolution integrals and Equation (22) holds true for any value of the transformed parameter.

Analytical integration of the matrix coefficient in Equation (22) is not, in general, possible and therefore numerical quadrature must be used. One can distinguishes two basic cases of integrand behavior, non-singular and singular. In the former case, the distance r between the field point ξ and integration point x on the surface of the element is never zero. In the former case, ξ. coincides with one of the integration points and r becomes zero.

For the non-singular case, one can use Gauss-Legendre quadrature approach for deriving the integrals. For improving accuracy, an element is divided into sub-elements [5,7].

For the singular case, one distinguishes here between behaviors of the displacement kernel, which is of order *log(r)*, and that of the traction kernel, which is of order r^{-1} (in 2D), as r tends to zero. In the displacement kernel case, the singularity is mild enough to allow recycling of the non-singular integration scheme, but special logarithmic one. The integral in the traction kernel case, however, exists only in a Caushy principal value (CPV) sense due to the presence of the strong singularity. Of course there is some indirect methods, like using rigid body motion approach, and deriving diagonal (singular) parts, in terms of off-diagonal (non-singular) terms. This approach can be extended to dynamics, because the behavior of the transient kernels as their arguments tend to zero, is identical to

the behavior of the corresponding static kernels for $r \to 0$ (and for transformed domain as well).

After imposing of boundary conditions, Equation (22) converts to a system of linear algebraic equations:

$$[A]\{X\} = [B] \tag{23}$$

and solving this equation gives us the boundary unknowns $\{X\}$.

Wave Scattering by Surface Irregularity

Wave scattering by ground surface topography such as canyons, are of major importance in earthquake engineering field. For deriving the governing equation, one can assume the total displacement field u as the sum of the free field u^f and scattered field u^s, i.e.;

$$u_i = u_i^f + u_i^s \tag{24}$$

The free field motion designates the wave field in the half-space in the absence of the irregularity, i.e. the sum of incident field and the reflected field from the boundary surface [4]. The scattered field motion satisfies the radiation condition at infinity. Then, one can write the boundary integral equation for the scattered field u_i^s as (in frequency domain):

$$\int_{S_a+S_b} \overline{F}_{ij}\overline{u}_j^s ds - \int_{S_a+S_b} \overline{G}_{ij}\overline{t}_j^s ds = C_{ij}\overline{u}_{ij}^s \tag{25}$$

where S_a and S_b are the surfaces of the half plane and the canyon, respectively (**Figure 1**).

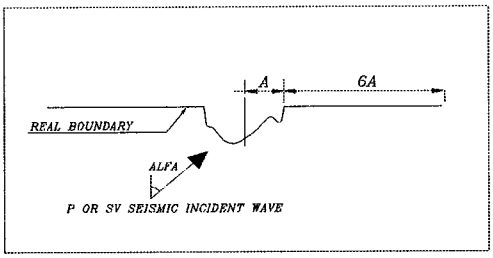

Figure 1. Half-space geometry under seismic incident waves

According to the boundary conditions on S_a and S_b;

$$\begin{aligned} \overline{t}_i &= \overline{t}_i^f = \overline{t}_i^s = 0 \quad \text{on} \quad S_a \\ \overline{t}_i &= \overline{t}_i^f + \overline{t}_i^s = 0 \quad \text{on} \quad S_b \end{aligned} \tag{26}$$

Equation (24) can be written as:

$$\int_{S_a+S_b} \overline{F}_{ij}\overline{u}_j^s ds + \int_{S_b} \overline{G}_{ij}\overline{t}_j^f ds = C_{ij}\overline{u}_{ij}^s \tag{27}$$

After discretization and collocation procedure:

$$[\overline{F}]\{\overline{u}^s\}=[\overline{G}]\{\overline{t}^s\} \tag{28}$$

and the vector $\{\overline{u}^s\}$ of the nodal scattered displacements on the surface S_a and S_b will be determined. The total displacement field can then be computed from Equation (23). Finally, the same approach can apply for time domain problems, considering the time-convolution integrals in this case.

Half-Space Analysis Using Fictitious Boundaries

According to the theoretical feature of double-layer potential functions, an indirect BEM is introduced [3,5]. In fact, a direct approach of converting the governing equations by these type of functions is not applied, but existing the similarity between a jump term in both of the methods (BEM and double-layer potentials), concluded to the proposed indirect BEM for solving some mathematical problems in direct BEM.

This proposed method is based on using a fictitious boundary, parallel and near the real one, and separating the placement of source and receiver points (**Figure 2**). The collocation scheme will be done on the real boundary, and integration on the fictitious one. Then, the distance between source and receiver points never tends to zero, and the singularity problem will vanish. But the most important problem will be the location of this fictitious boundary, regarding to accuracy of the results and then efficiency of the proposed indirect method. Case studies with different shapes of canyon, different kind of incident waves, different angle of incidences, and different time steps and frequency contents of incident wave are done for deriving the safe zone for placing that fictitious boundary. The proposed method is applied in both frequency and time domains BEM, and the safe zone for placing of the fictitious boundary in each case is derived. Of course there are some analytical methods for checking the accuracy of solutions and then deriving the best limits for the fictitious boundary, but according to a better feeling about the behaviour of physical parameters (e.g. displacements), a numerical trial error method is preferred.

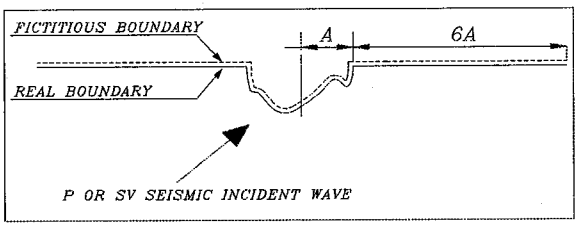

Figure 2. Half space domain with fictitious boundary under seismic wave

CASE STUDIES AND RESULTS

BEM in Frequency Domain

In this part of study, according to the abovementioned formulations, canyons under seismic waves are analyzed. First of all, half-space analyses in frequency domain are investigated. Results of direct BEM are verified by closed form solutions, and then case studies for deriving the safe zone according to the accuracy of proposed IBEM in transformed domain are implemented. In the second stage, the same procedure for determining the safe zone for proposed IBEM in time domain will be presented.

To gauge the accuracy and range the applicability of developed BEM for half-space in frequency domain, a semi-cylindrical canyon of radius R is considered. The analytical results for this case are presented by Cao & Lee (1990) [3]. Several runs were made with different combinations of angle of incidence θ and frequency content of wave. In all of the examples, the following dimensionless frequency parameter η is used:

$$\eta = \frac{\omega a}{\pi C_2} \tag{29}$$

Meanwhile, a Poisson ratio of ν=0.25 is assumed.

For illustration purpose, values of total displacements, i.e. the horizontal ($|u_x|$) and vertical ($|u_y|$) components, plotted versus the dimensionless distance x/R and the dimensionless frequency, η, for angle of incidences α=0,30, 60 and 85° are presented. Table 1 gives the surface displacement amplitudes of the half-space for incident P wave and for various angles of incidence. In these figures, the displacement amplitudes on the surface of the canyon are plotted along the horizontal x-axis in the interval $-1 \le x/R \le 1$.

Table 1. Displacement component values

Angle of incidence, α, degree)	$\|u_x\|$	$\|u_y\|$
0	0	2
30	1.12	1.69
60	1.73	1.00
85	0.97	0.35

As seen from **Figure 3**, good agreements were found in all of the applied frequencies. The complexity of the surface displacements, caused by the presence of the semi-circular canyon, increases with increasing frequency, η Actually, long ness of wavelength λ at small frequencies, compared with the radius of the canyon R, causes this phenomenon.

On the other hand, the effect of the angle of incidence α on the resulting displacement pattern is illustrated. As α increases from 0 to 85°, the complexity of the amplitudes of surface displacements increases for region x/R<-1. As seen from figure 3, due to the mode conversion exhibited by P wave incidence, both of the horizontal and vertical components of displacement can be larger than the free field amplitudes behind the canyon (x/R>1). Then, one cannot describe a permanent shadow zone behind of canyon.

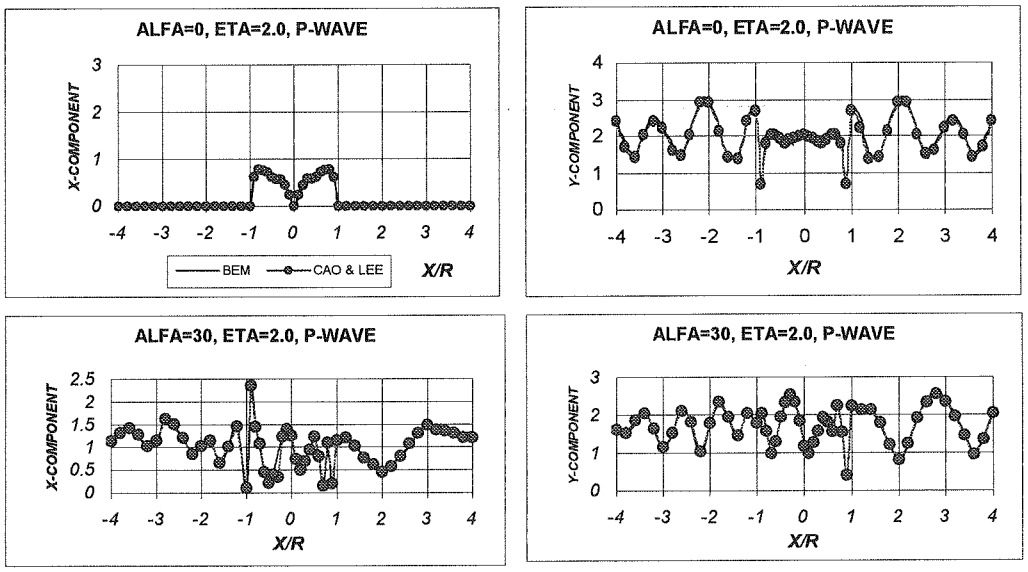

Figure 3. Semi-circular canyon under P wave

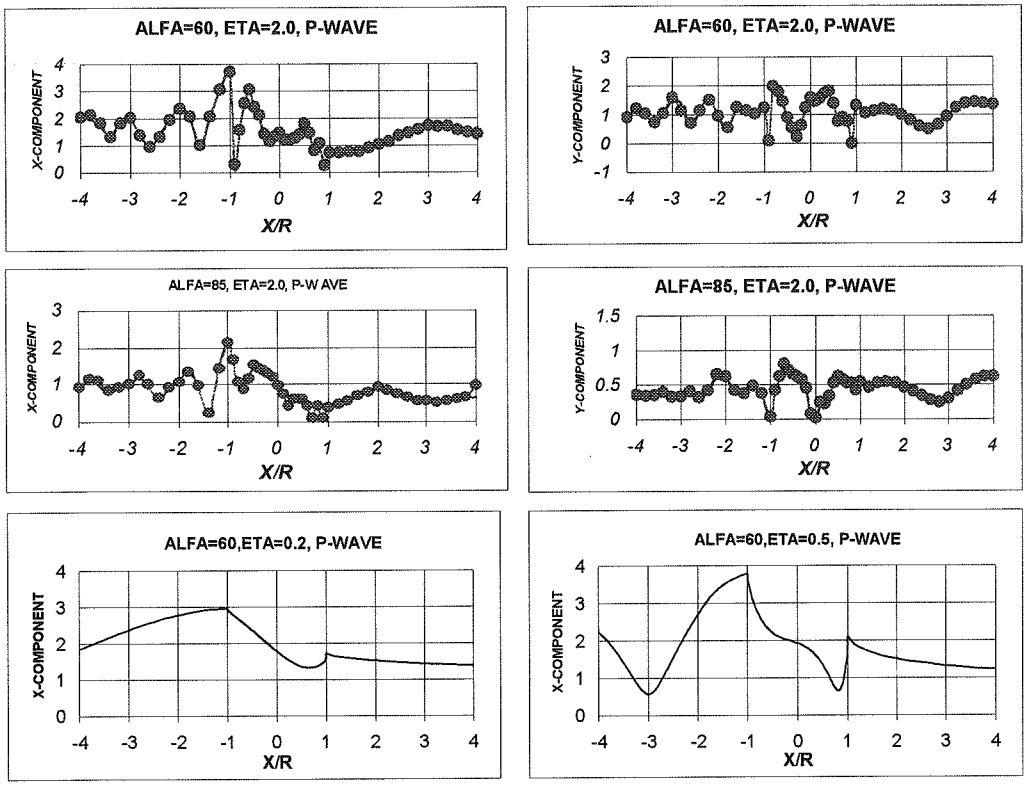

Figure 3. Semi-circular canyon under P wave (continued)

BEM in Time Domain

Based on the formulations mentioned in time domain BEM, the approach is developed in this domain using relative displacement and traction fundamental solutions. The main difference between present case and transformed domain, is the time convolution property of integrals. Using time translation property of fundamental solutions, a step by step integration procedure should be consider, and it causes a longer solving time, according to the former case. Analyses showed that a time step lower than the necessary time for sweeping one forth of the smallest element in the model, could be sufficient.

In this part of study, two shapes of canyons are analyzed under harmonic incident waves. On the other hand, regarding to the lack of such an analysis for verification, the results are compared with the converted results from transformed domain analysis. In **Figure 4** this comparison is showed for semi-circular and semi-elliptical canyons. As one can distinguishes, except the first steps that time domain program needs to get to equilibrium, there is a good agreement between these results.

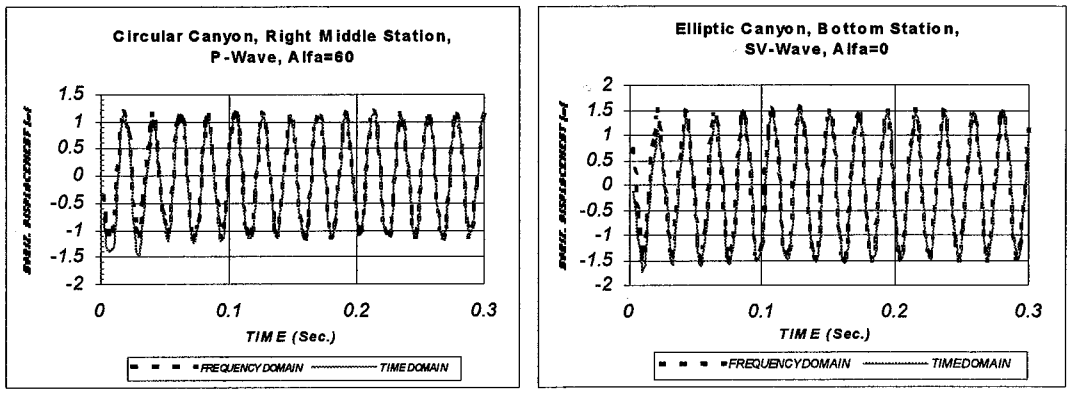

Figure 4. Comparison of results between F.D. and T.D. BEM

IBEM in Frequency Domain

According to the abovementioned procedure illustrated in indirect BEM, different case studies for gauging the accuracy of the method in transformed domain were analyzed. In each study, dimensionless response (the ratio of average results from BEM to that from proposed IBEM) is plotted versus a dimensionless distance parameter *d/R*; where d is the distance between real and fictitious boundaries, and *R* is the half-width of canyon. This procedure is done for different shapes of canyon (**Figure 5**). Then, the safe zone for placement of fictitious boundary will be around where the dimensionless displacement parameter is about unity (average results are derived from bottom and topside points).

Figure 6 shows the diagram related to a semi-circular canyon under in-plane seismic waves. One can distinguish a noticeable zone for fictitious boundary with agreeable accuracy. To have generality, canyons with semi-elliptical, full-convex, and concave-convex arbitrary shapes were analyzed. **Figure 6** illustrates that this method works well in all of those applied situations, and a limit between 0.002 to 0.010 times of the half-width of the canyon, is a proper place for the safe zone according to the accuracy of the results.

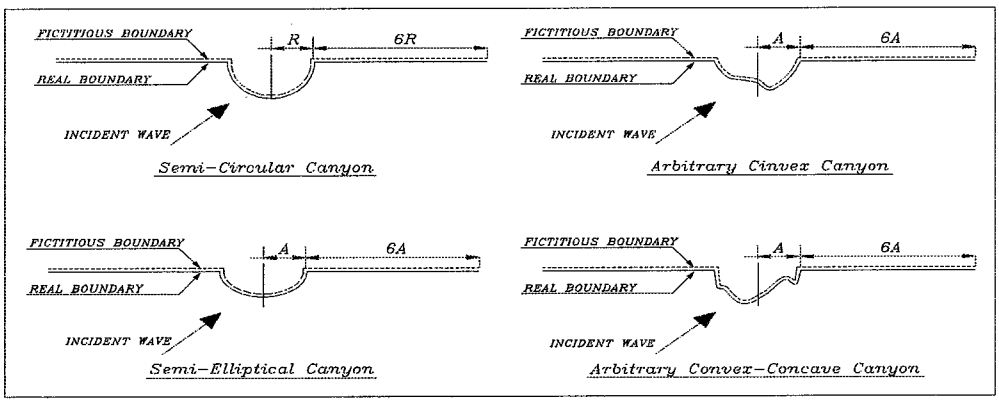

Figure 5. Different shapes of canyons with fictitious boundary under seismic wave

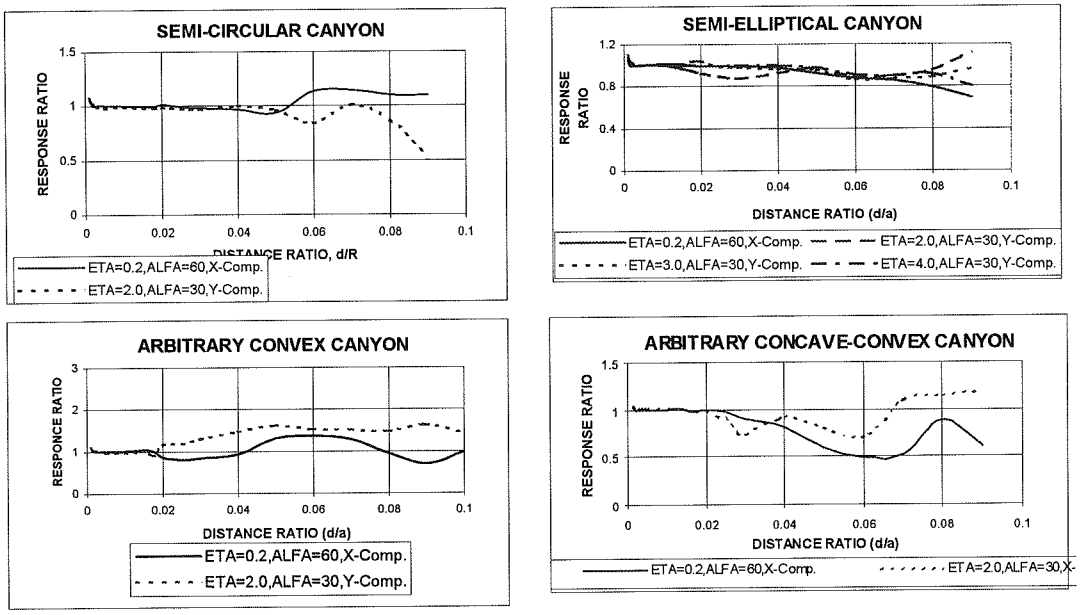

Figure 6. Indirect Analysis Results with IBEM

IBEM in Time Domain

A same indirect procedure with a fictitious boundary is adopted for gauging the accuracy and efficiency of proposed IBEM in time domain. The analysis results for two different shapes of canyons are shown in figure 7. A semi-cylindrical canyon and a full-convex arbitrary shape canyon are adopted for this part of study, and accuracy is gauged in different time steps. Again, a dimensionless displacement parameter is plotted versus dimensionless distance *d/R*. For generality, the results are checked in different points of the canyons and different time steps, from the first till the end. As seen in the diagrams, the method has good efficiency in time domain as well, and a limit between 0.002 to 0.009 times of half-width of the canyon, can be considered as the safe zone for such a half-space problem in time domain.

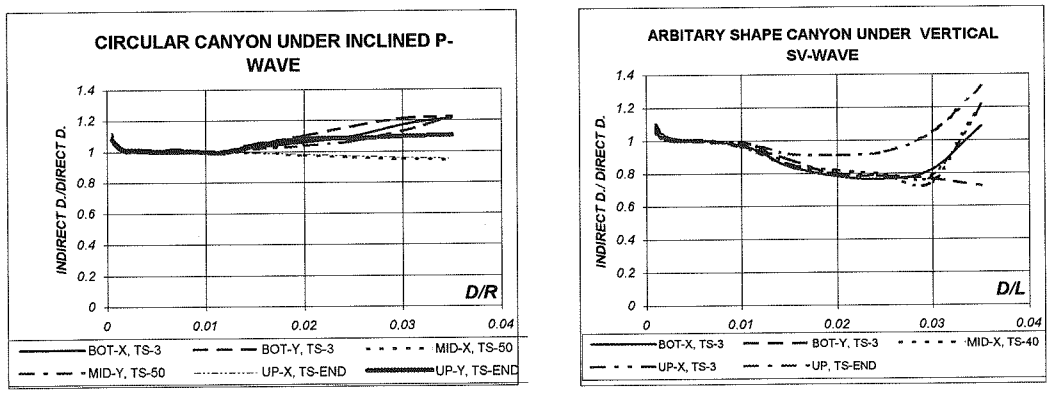

Figure 7. Appling IBEM in time domain

CONCLUSIONS

Based on the approach of boundary integral equations, half-space domains are analyzed under seismic incident in-plane waves, both in time and frequency domains. On the other hand, using a fictitious boundary near the real one, an indirect BEM is proposed to vanish the singularity problem in the direct method. This approach checked for both domains, and the case studies showed that it is efficient for solving this kind of problems. For both transferred and time domain problems, the safe zone for placing the fictitious boundary according to the accuracy of results, are derived with case studies by different canyon shapes and incident wave properties (angle of incidence and frequency content). For frequency domain problems, this zone is between 0.002 to 0.010 times of the half width of the canyon, and in time domain problems it is between 0.002 to 0.009 times of that.

AKNOWLEDGMENT

The authors wish to thank Professor Kazu Konagai from IIS, Tokyo University in Japan for his great help, advice, and encouragement during this work.

REFERENCES

1. Banerjee, P.K., *The boundary element method in engineering*, mc. Graw Hill, 1981.

2. Boore, D.M., *A note on the effect of simple topography on seismic SH waves*, Bull. Seism. Soc. Am., 62, 275-284, 1972b.

3. Cao, H. and Lee, V.W., *Scattering and diffraction of plane P waves by circular cylindrical canyons with variable depth-to-width ratio*, soil Dyn. Earth. Eng., 1990, 9.

4. Graff, K.F., *Wave motion in elastic solids*, Columbus; Univ. of Ohio Press, 1975.

5. Khoshdel, S.H., *Indirect boundary integral method for half-space analysis under seismic incident waves*, PhD Dissertation, Tehran Univ., IRAN, December 2001.

6. Lee, V.W., *Displacements near a three-dimensional hemispherical canyon subjected to incident plane waves*, USC Report, CE 78-16, 1978.

7. Manolis, G.D. and Beskos, D.E., Boundary *Element Method in Elastodynamics*, Prentice Hall,1988.

8. Sanchez-Sesma, F.J. and Rosenblueth, E., *Ground motion at canyons of arbitrary shape under incident SH waves*, Earth. Eng. Struc. Dyn., 1974, 7, 441-450.

9. Shah A.H. and Wang K.C., *Diffraction of plane SH waves in a half-space*, Earthqu. Eng. Struc. Dyn., 10, 519-528, 1982.

10. Smith, W.D., *The application of finite element analysis to body wave propagation problems*, Geophys. J. 44, 1977.

11. Trifunac, M.D., *Scattering of plane SH waves by a semi-cylindrical canyon*, Earthqu. Eng. Struc. Dyn., 1, 267-281, 1993.

12. Wong, H.L. and Trifunac, M.D., *Scattering of plane SH waves by a semi-cylindrical canyon*, Int. J. Earth. Eng. Struct. Dyn., 1974,3,159-169.